Supporting Information: Wind-Driven Emissions of Coarse Mode Particles from an Urban Environment

Markus D. Petters[1], Tyas Pujiastuti[1], Ajmal Rasheeda Satheesh[1], Sabin Kasparoglu[1], Bethany Sutherland[1], and Nicholas Meskhidze[1]

[1]Department of Marine, Earth, and Atmospheric Sciences, North Carolina State University, Raleigh, NC 27695, USA.

Correspondence to: Markus D. Petters (mdpetter@ncsu.edu)

1 Intercomparison of radiosonde and ground-based meteorological station RH

Figure S1 shows a scatterplot comparing the interpolated radiosonde RH measured at 8m and RH measured by the MET system. The interpolated sonde product generates a time series based on a discrete number of sonde launches during the day. The slope of the regression line is 1.05. Approximately 68% of the data fall within the interval RH ± 7%, which characterises one standard deviation of the variability.
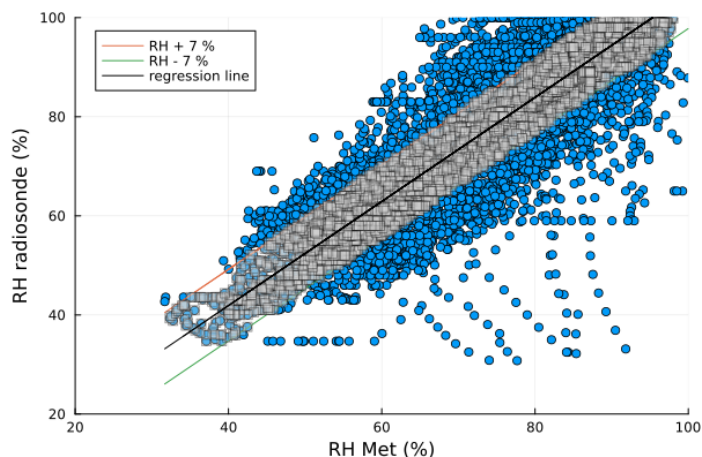

Figure S1: Comparison of interpolated radiosonde RH measured at 8m and RH measured by the MET system. The shaded area corresponds to ±7% in RH and was selected such that 68% of the data points fall between RH + 7% (red) and RH -7% (green) model lines.

2 Relationship between backscatter and number flux

As given in the main text, the eddy-covariance number flux $<w'N'>$ can be obtained from the eddy-covariance backscatter flux $<w'\beta'>$ via

$$\left\langle w'N'\right\rangle = \left\langle w'\beta'\right\rangle / \left(\frac{\partial\beta}{\partial N}\right)_{S} - \left(\frac{\partial\beta}{\partial S}\right)_{N} / \left(\frac{\partial\beta}{\partial N}\right)_{S}\left\langle w'S'\right\rangle \tag{S1}$$

where the partial derivatives $(\partial\beta/\partial N)_S$ and $(\partial\beta/\partial S)_N$ denote the sensitivity of backscatter to number concentration and saturation ratio, and $<w'S'>$ is the saturation ratio flux. The partial derivative $(\partial\beta/\partial N)_S$ equals the slope of the regression lines between β and N shown in Figure 4, i.e.,

$$\beta(S) = m(S)N + c(S) \tag{S2}$$

where $m(S) = (\partial\beta/\partial N)_S$ is the slope, N is the number concentration, and $c(S)$ is the intercept. As shown in Figure 4, m(S) is evaluated in intervals [S;S+0.05]. Eq. (S2) can be used to evaluate $(\partial\beta/\partial S)_N$

$$\left(\frac{\partial\beta}{\partial S}\right)_{N} = \left(\frac{\partial m(S)}{\partial S}\right)_{N}N + \left(\frac{\partial c(S)}{\partial S}\right)_{N} \tag{S3}$$

As shown in Figure 4m, main text, the slope $m(S)$ is approximately invariant with S for $0.4 < S < 0.6$ and increases with S for larger saturation ratios. The saturation ratio flux is given by (Vong et al., 2004)

$$<w'S'> = \frac{<w'q'>}{q_{sat}} - \frac{<w'T'>SL_v}{R_vT} \tag{3}$$

where $<w'q'>$ is the water vapour turbulent flux, q_{sat} is the mean specific humidity at saturation, $<w'T'>$ is S is the mean ambient air saturation ratio, L_v is the latent heat of vaporisation of water and R_v is the ideal gas constant for water vapour. Using the definitions of latent heat flux $Q = L_v\rho <w'q'>$ and sensible heat flux $H = c_p\rho <w'q'>$, where c_p is the specific heat capacity and ρ the density of air, Eq. (3) becomes

$$<w'S'> = \frac{Q}{\rho L_v q_{sat}} - \frac{HSL_v}{\rho c_p R_v T} \tag{4}$$

Eq. (4) is evaluated as follows. The mean saturation ratio and temperature are obtained at LIDAR height z using the interpolated sonde product. Density at the LIDAR height is evaluated as follows. The measured surface pressure is reduced according to the scale height equation $p(z) = p_0\exp(-z/8000m)$, where $p(z)$ is the pressure at height z and p_0 is the surface pressure. The density is obtained using the pressure at height z and the virtual temperature at height z. Specific humidity at height z is obtained from the estimated temperature and saturation ratio at height z. Latent and sensible heat fluxes are obtained from the ECOR system at the surface. The height dependence of these quantities (Behrendt et al., 2020) is not taken into account here. The saturation flux values vary between -0.25 and 0.25 cm s^{-1}. Typical values for the ratio

$(\partial\beta/\partial S)_N/(\partial\beta/\partial N)_S$ are up to ~40 cm^{-3} for the $D = 0.53$ µm cutoff. Thus, the estimated maximum contribution from subtrahend to the flux is ~10 cm^{-2} s^{-1}.

4 Exploratory statistical analysis

Figure S2 summarises the statistical relationship between the observed fluxes and potential explanatory variables.
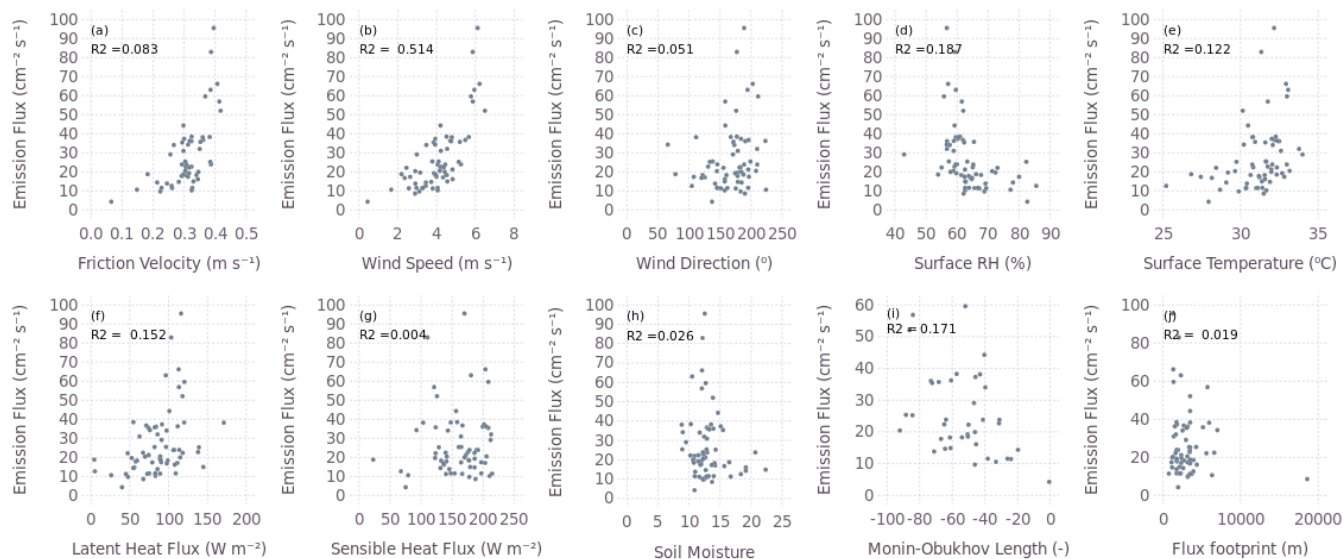

Figure S2: Scatter plots for (a) friction velocity, (b) wind speed, (c) wind direction, (d) surface RH, (e) surface temperature, (f) latent heat flux , (g) sensible heat flux and (h) soil moisture, (i) Monin-Obukhov length, (j) flux footprint versus number fluxes. Pearson correlation coefficients (R^2) values are given in the plots.

References

Behrendt, A., Wulfmeyer, V., Senff, C., Muppa, S. K., Späth, F., Lange, D., Kalthoff, N., and Wieser, A.: Observation of sensible and latent heat flux profiles with lidar, Atmospheric Meas. Tech., 13, 3221–3233, https://doi.org/10.5194/amt-13-3221-2020, 2020.

Fairall, C. W.: Interpretation of eddy-correlation measurements of particulate deposition and aerosol flux, Atmospheric Environ. 1967, 18, 1329–1337, https://doi.org/10.1016/0004-6981(84)90041-6, 1984.

Kowalski, A. S.: Deliquescence induces eddy covariance and estimable dry deposition errors, Atmos. Environ., 35, 4843–4851, https://doi.org/10.1016/S1352-2310(01)00270-9, 2001.

Vong, R. J., Vickers, D., and Covert, D. S.: Eddy correlation measurements of aerosol deposition to grass, Tellus B Chem. Phys. Meteorol., 56, 105–117, https://doi.org/10.3402/tellusb.v56i2.16414, 2004.